Identification of Lipid Aggregate Structures on TiO_2 Surface Using Headgroup IR Bands

Cuihong Jiang, Alla Gamarnik, and Carl P. Tripp*

Laboratory for Surface Science and Technology and Department of Chemistry, University of Maine, Orono, Maine 04469

Received: September 1, 2004; In Final Form: November 26, 2004

Attenuated total reflection-Fourier transform infrared (ATR-FTIR) spectroscopy was used to study the nature of the dipalmitoylphosphatidylcholine (DPPC) aggregated structures adsorbed on TiO_2. DPPC molecules were assembled on TiO_2 using Langmuir−Blodgett (LB) deposition methods or by directly flowing the DPPC liposome solution across the TiO_2-coated ATR crystal. We found that there is a direct correlation between the intensity and frequency position of the zwitterionic headgroup IR bands and the nature of LB films. Specifically, we have shown that the bands due to PO_2^- modes are sensitive to changes in the degree of hydration of the LB films and that the symmetric deformation vibrational mode (δ_s $^+N-CH_3$) is sensitive to interaction with oppositely charged surface sites. Using this information, we found that the liposomes adsorbed on TiO_2 remain intact as vesicles and that the vesicles are stable and not removed in flowing water. We have also shown that the antisymmetric deformation vibrational (δ_{as} $^+N-CH_3$) modes are sensitive to changes in lateral−lateral DPPC interactions. This information was used to show that there is a lateral interaction between each positively charged $^+N(CH_3)_3$ headgroup and negatively charged PO_2^- headgroup of the adjacent DPPC molecule in the adsorbed vesicles and LB films. This study provides a framework for the use of this IR technique in studies of adsorption and transport of molecules across membrane interfaces.

Introduction

Phospholipid vesicles (liposomes) have received considerable attention in recent years because of their use as a simplified model of biological membranes and delivery systems.[1−5] They consist of a bilayer of amphiphilic phospholipid molecules in the shape of a spherical shell, separating an intracellular liquid volume from the extracellular space. The vesicles are often bound to a surface to study the bio-reactions occurring at the membrane interface. The morphology of lipid aggregates on solid surfaces (silica, mica, or titania) has been studied by various techniques, such as quartz crystal microbalance (QCM),[6−9] surface plasmon resonance,[9] light scattering,[10,11] atomic force microscopy (AFM),[12−14] and optical microscopy.[15] To the best of our knowledge, infrared (IR) spectroscopic studies of vesicles bound to surfaces have not been reported.

Recently, we have established an IR spectroscopic approach that can be used to identify mixed surfactant structures formed on metal oxide surface in aqueous solutions.[16] The technique is based on the use of attenuated total reflection-Fourier transform infrared (ATR-FTIR) spectroscopy in which a ZnSe crystal is coated with high surface area TiO_2 particles. One advantage of using an IR method is that the amount of each adsorbate can be monitored separately when mixtures of surfactants and polymers are adsorbed on TiO_2. Furthermore, the use of high surface area TiO_2 particles made it possible to detect the weak, yet information-rich, headgroup IR bands of surfactants. It is the headgroup bands that provide the important structure information on the mixed surfactant architectures. It is generally agreed that vesicles remain intact when adsorbed on TiO_2 because the vesicle−surface interactions are weak.[6−8,17,18] Therefore, a similar investigation of the zwitterionic headgroup IR bands for phosphotidylcholine (PC) vesicles adsorbed on TiO_2 using this ATR-FTIR method could provide important structural information on the nature of the liposome architecture when bound to a surface.

In this present work, we establish the correlation between the IR bands of dipalmitoylphosphatidylcholine (DPPC) adsorbed on TiO_2 and the nature of the aggregated structure. The particular focus is on the zwitterionic headgroup bands. The structure of the DPPC aggregates is deduced by comparing the spectra obtained from Langmuir−Blodgett (LB) DPPC films and DPPC vesicles deposited on TiO_2. The advantage of LB film deposition is that this method is capable of assembling individual molecules layer-by-layer into a highly organized molecular architecture. A basic understanding of the DPPC structure adsorbed on TiO_2 from the analysis of the headgroup bands provides a framework for the use of IR technique in studies of adsorption and transport of molecules across membrane interfaces.

Experimental Section

Materials. The solvents including $CHCl_3$ and CH_3OH were purchased from Aldrich and used as received. Deionized water (18 MΩ) was obtained from a Milli-Q purification system. Dipalmitoylphosphatidylcholine (DPPC), obtained from Avanti Polar Lipids, Inc., Alabaster, AL, with purity of 99%, was used without any further purification. The chemical structure of DPPC is shown in Figure 1. Fumed titanium dioxide (P25, surface area of 50 m^2/g) was obtained from Degussa and has a measured isoelectric point (IEP) of pH 6.5. The P25 is nonporous with a primary particle size of about 15 nm diameter forming larger clusters of about 200 nm diameter in size.

Substrate Pretreatment. The ZnSe internal reflection element (IRE) was obtained from Harrick Scientific and has dimensions of 50 × 10 × 2 mm, with 45° beveled faces. Titania-

* To whom correspondence should be addressed. Phone: (207) 581-2235. Fax: (207) 581-2255. E-mail: ctripp@maine.edu.

10.1021/jp046042h CCC: $30.25
Published on Web 02/18/2005

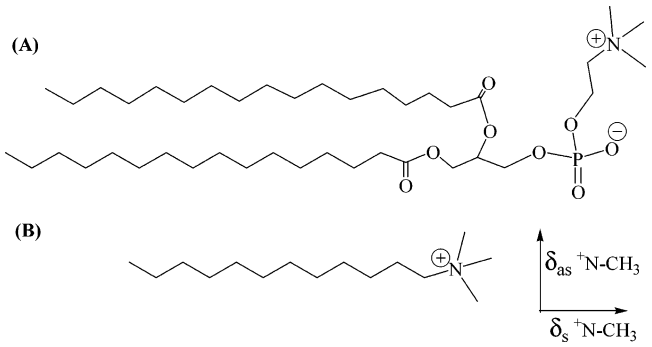

Figure 1. Chemical structures of DPPC (A) and CTAB (B) indicating the direction of the transition dipole moment vectors for $^{+}N-CH_3$ bending modes for the $^{+}N(CH_3)_3$ headgroup of both DPPC and CTAB.

coated ZnSe crystal was used as the substrate for most of the work in this study. The procedure for generating a stable TiO_2 powder film on ZnSe IRE's is described elsewhere.[19] A TiO_2 layer was prepared by depositing a 200 μL aliquot of a suspension of 30 mg of P25 TiO_2 in 25 mL of methanol onto a ZnSe IRE. After evaporation of the methanol, a uniform (approximately 500 nm thickness) TiO_2 film is formed that is stable, showing no loss of powder to flowing aqueous solutions containing polyelectrolytes and surfactants over a pH range of 2−10.[19] AFM analysis shows that the TiO_2 film has a surface rms roughness of about 80 Å. The SEM micrograph of the films[19] shows that the films are highly cracked with crevices as large as 2.5 μm across. These cracks are large as compared to the diameter of the liposomes and provide a route for the liposomes to penetrate into the TiO_2 layer.

Dry Multilayer Films. DPPC multilayer film was prepared by uniformly spreading ~400 μL of a 25 mg/mL chloroform solution on one side of a ZnSe ATR crystal followed by gradual evaporation of the solvent.

Vertical Langmuir−Blodgett (LB) Deposition of Lipid Monolayers. An automatically controlled Langmuir film balance (KSV2000, KSV Instruments Ltd., Finland) equipped with a platinum Wilhelmy plate was used to deposit the lipid monolayers on TiO_2. For all experiments, deionized water was used as the subphase, spectroscopic grade chloroform (Aldrich) was used as the spreading solvent, and the temperature was maintained at 22 ± 1 °C. The cleanliness of the trough and subphase was ensured before each experiment by aspirating the surface of the subphase. The surface was deemed to be clean when the surface pressure fluctuation was found to be less than 0.03 mN/m during a compression cycle. A 50 μL chloroform sample containing phospholipids was then spread on the subphase surface using a microsyringe (Hamilton Co.). After evaporation of the chloroform (~30 min), DPPC at the air/water interface was continuously compressed at a rate of 10 mm/min until the surface pressure reached 45 mN/m, which is the compact monolayer region in the isotherm of DPPC.[20] This compressed monolayer was transferred by raising the TiO_2-coated IRE from the subphase through the air/water interface. The surface pressure was maintained constant during the transfer process. Multilayer samples were obtained by successively dipping the substrate through the monolayer while simultaneously keeping the surface pressure constant.

Given that the LB deposition is not on a "flat" surface but rather a TiO_2 particulate film with a surface roughness of about 80 Å, it is unlikely that uniform "defect-free" layers are deposited. The final sample characterized by ATR-FTIR could thus contain uncovered areas and stacked bilayers, even though the transfer ratio data and intensity of IR bands suggest that

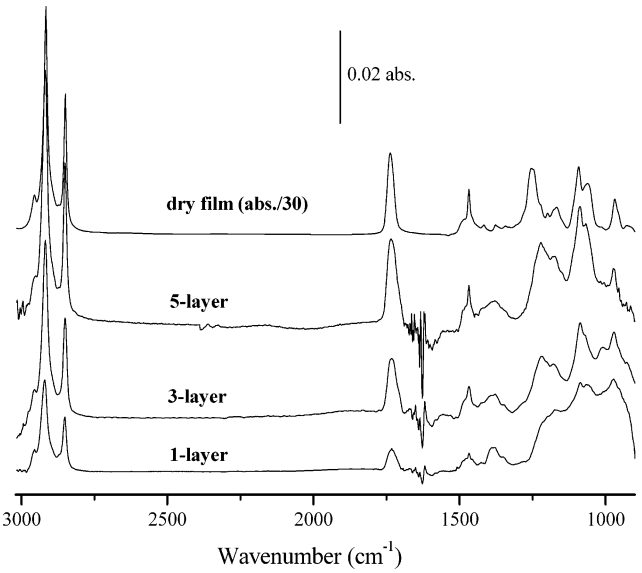

Figure 2. ATR spectra of lipid molecules assembled on TiO_2 surface after 1, 3, and 5 LB cycles, labeled as "1-layer", "3-layer", and "5-layer", respectively. The spectrum of a DPPC "dry film" on ZnSe crystal is provided for comparative purposes.

the samples prepared are roughly "monolayer", "three layers", and "five layers", respectively. Nevertheless, the 1, 3, and 5-layer designations are used to provide a qualitative interpretation of the spectra.

Liposome Preparation. Unilamellar liposomes of uniform size were prepared by the method described elsewhere.[21] In brief, a lipidic film was formed by rotary evaporation of a lipid/$CHCl_3$ (200 mg in 6 mL) solution. The film was then hydrated overnight in 20 mL of deionized water followed by an 8-fold passage through 200 nm polycarbonate membranes. The concentration of liposome is about 7 g/L with a vesicle size of approximately 200 nm diameter as measured on a Malvern Zetasizer 3000 system.

Flow-Through ATR Procedure. A TiO_2-coated ZnSe IRE was mounted into the standard ATR liquid flow cell obtained from Harrick. A peristaltic pump with a flow rate of 3 mL/min was used to flow water and the DPPC solutions across the TiO_2-coated ZnSe IRE. In a typical experiment, the deionized water, adjusted to pH 8.5 with NaOH, was flowed for 2 h across the IRE. A reference spectrum was then recorded. Next, a DPPC liposome solution at pH 8.5 was introduced into the system. Spectra were recorded as a function of time, and the DPPC was flowed continuously until no significant changes were observed in the IR spectrum. It is noted that the DPPC vesicles adsorbed on TiO_2 were stable to flowing solutions of water at pH 8.5. Flowing water at pH 8.5 for 2 days did not result in any decrease in intensity of bands due to DPPC adsorbed on the TiO_2-coated ZnSe IRE.

Fourier Transform Infrared Spectroscopy. All infrared spectra were recorded on a Bomem MB-series FTIR spectrometer equipped with a liquid N_2-cooled mercury cadmium telluride (MCT) detector. Typically, 100 scans were co-added at a resolution of 4 cm^{-1}.

Results and Discussion

IR Spectra of LB-Deposited DPPC Layers. In our first set of experiments, controlled amounts of DPPC were deposited on the TiO_2 surface using LB methods. Figure 2 shows the ATR spectra of LB-deposited lipid molecules onto the TiO_2 surface. For comparative purposes, the spectrum of a DPPC dry film

TABLE 1: Assignment of Major IR Bands for DPPC Layers on TiO_2

wavenumber (cm^{-1})	assignment[22]
2957	terminal CH_3 antisymmetric stretch
2920	chain CH_2 antisymmetric stretch
2873	terminal CH_3 symmetric stretch
2851	chain CH_2 symmetric stretch
1734	ester C═O stretch
1468	CH_2 scissor
1420	CH_2 bend
1396	$^+N-CH_3$ symmetric deformation
1380	terminal CH_3 symmetric bend
1223	PO_2^- antisymmetric stretch
1173	ester C−O−C antisymmetric stretch
1088	PO_2^- symmetric stretch
1068	ester C−O−C symmetric stretch
970	$^+N-(CH_3)_3$ antisymmetric stretch

TABLE 2: CH_2 Band Frequency and fwhh Values

DPPC samples	frequency (fwhh)/cm^{-1}	
1-layer	2851 (14)	2919 (20)
3-layer	2850 (13)	2919 (19)
5-layer	2849 (12)	2918 (18)
dry film	2848 (11)	2916 (15)
vesicles	2849 (12)	2918 (17)

(0.02 mg/mm^2) is also shown in Figure 2. The assignments of each band in the spectra are listed in Table 1.[22] The first feature to note is the quality of the LB spectra in terms of signal-to-noise. This is a direct result of using high surface area TiO_2 particles as the adsorbate. We found that a spectrum of intensity similar to that of the 1 layer LB deposition on TiO_2 shown in Figure 2 would require the equivalent of ∼50 layer LB depositions on a bare ATR crystal (spectrum not shown). The most prominent features can be conveniently divided into four spectral regions: bands between 2960 and 2850 cm^{-1} assigned to C−H stretching modes, a C═O band near 1730 cm^{-1}, $^+N-(CH_3)_3$ headgroup bands near 1400 cm^{-1}, and phosphate headgroup bands at 1223 and 1088 cm^{-1}.

(a) Hydrocarbon Chain Modes. The CH_2 asymmetric stretching mode near 2920 cm^{-1} and the symmetric mode near 2850 cm^{-1} are generally the strongest bands in the spectra of lipids. The correlation between the frequency position and full-width-at-half-height (fwhh) values of the CH_2 stretching modes and the packing density of the hydrocarbon tails is well established.[22−24] A shift to lower frequency is accompanied by a lower fwhh indicative of more highly packed structure. Table 2 shows the band positions and the corresponding fwhh values of these CH bands for different samples. As compared to the DPPC dry film spectrum, each LB spectrum in Figure 2 shows CH_2 stretching modes at higher frequency and larger fwhh. This higher frequency of the CH_2 stretching bands suggests a more conformational disordered liquid phase of CH_2 long chains in the LB monolayers.

Among the LB spectra, the trend shows that the CH_2 bands become sharper and shift to lower frequency with an increase in the number of layers on the TiO_2 substrate. This shows that as more DPPC layers are successively assembled on the substrate, the molecules become more ordered. This should lead to a reduction in the amount of water between layers, and this is confirmed in the next section, in which spectra in the phosphate headgroup region are discussed.

(b) The Phosphate Headgroup Region. While there are subtle changes in the position and width of the CH_2 stretching bands of the methylene tail when comparing the three LB spectra in Figure 2, the headgroup region shows significant changes in relative intensities of various bands. Figure 3 is a replot of the

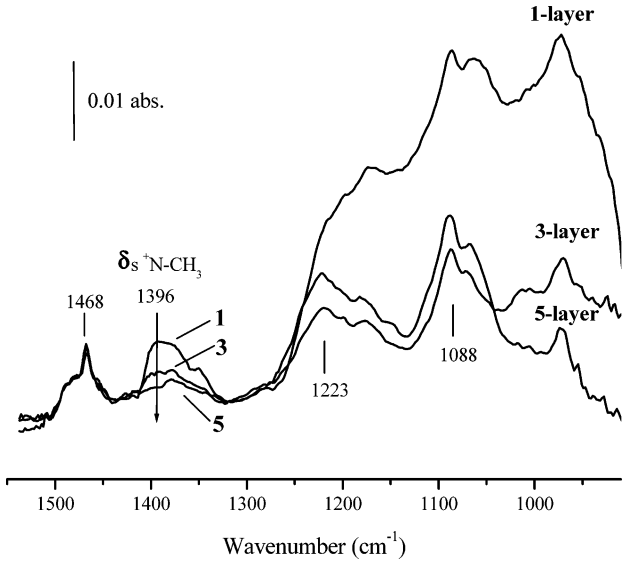

Figure 3. Relative intensity of the DPPC headgroup bands for 1, 3, and 5 LB layers on the TiO_2 surface. The spectra are scaled to the intensity of the CH_2 band at 1468 cm^{-1}.

spectra in the headgroup regions ($^+N(CH_3)_3$ and PO_2^-) for 1, 3, and 5 LB layers. For comparative purposes, the spectra are normalized to the CH_2 band at 1468 cm^{-1} (i.e., the spectra are normalized for the same amount of DPPC). The lower frequency region of spectra in Figure 3 contains bands at 1223 and 1088 cm^{-1}, assigned to vibrational modes due to the PO_2^- headgroups. In comparison to the dried DPPC film, the PO_2^- bands are broadened and shifted to lower frequency. The frequency of this band at ∼1223 cm^{-1} for 3- and 5-layer is about 30 cm^{-1} lower than the one obtained for the DPPC dry film spectrum (∼1254 cm^{-1}). This 30 cm^{-1} shift is indicative that the LB assembled lipid molecules are highly hydrated. It is generally agreed that the phosphate groups are the major sites for hydrogen binding of water.[23,25,26] H-bonding interactions in the hydrated films with water are known to significantly lower the frequency of the PO_2^- stretching modes.[22,25−27] Takenaka et al.[22,27,28] have studied the effect of hydration on the IR spectra of dried DPPC multilayers on an ATR crystal. They found the PO_2^- bands broadening with hydration, and they attributed this to incorporation of water into the DPPC layers. The effect of hydration is much more pronounced in our case in comparison to the study by Takenaka et al. because of the number of deposited layers used in their study. In our case, we found that an increase in the number of lipid layers on the surface results in an average decrease in the hydration level of those lipid molecules. The broadening of the PO_2^- bands is most dramatic for the 1 LB layer resulting in the disappearance of a discernible peak at 1223 cm^{-1}. This is not surprising as most of the lipid molecules in the first lipid monolayer are loosely packed and fully hydrated as the headgroups are exposed to the water. With deposition of 3 or 5 layers, the hydrophobic regions produced by the tail−tail interactions reduce the level of hydration of the DPPC headgroups. As a result, an increase in the number of LB layers leads to a decrease in the average hydration level. This is in agreement with the trend in the CH_2 stretching modes, which showed an increase in packing density with the number of LB layers deposited on the TiO_2. In this case, as more water surrounds the PO_2^- headgroups, there is more space available for the movement of the CH_2 tails.

(c) The $^+N(CH_3)_3$ Headgroup Region. The most prominent difference between the three spectra in Figure 3 is the change in the relative intensity of the symmetric deformation mode (δ_s

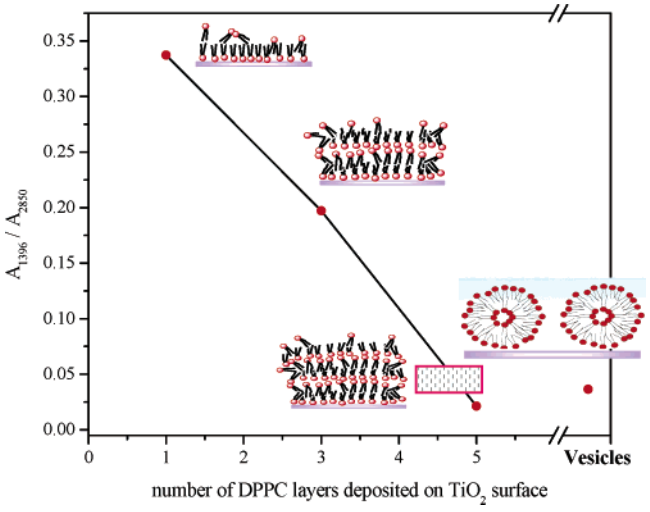

Figure 4. Relative intensity of the δ_s $^+N-CH_3$ band (A_{1396}/A_{2850}) as a function of the number of DPPC layers and DPPC vesicles deposited to the TiO_2. The pictures are provided as a guide to show the percentage of DPPC molecules directly interacting through the $^+N(CH_3)_3$ headgroups as a function of the number of "monolayers".

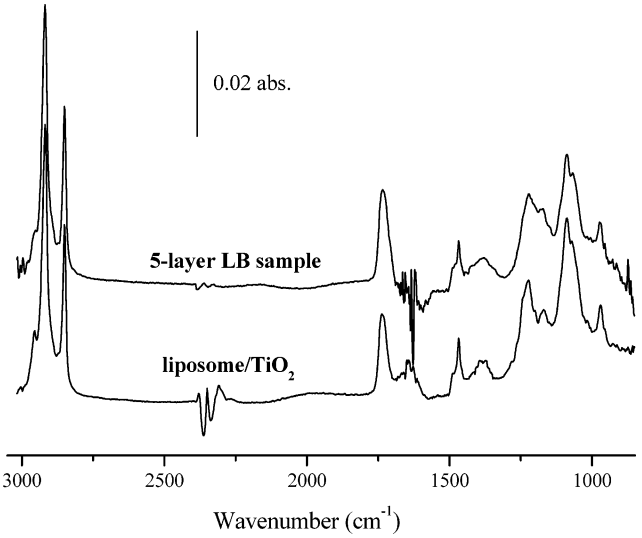

Figure 5. ATR spectrum of the lipid adsorbed on TiO_2 from a 5×10^{-3} M solution containing vesicles. The spectrum of the 5-layer LB sample is replotted for comparison.

$^+N-CH_3$) at 1396 cm^{-1}. The headgroup $^+N(CH_3)_3$ of 1396 cm^{-1} is interspersed with bands at 1468 cm^{-1} (δ CH_2), 1420 cm^{-1} ($\delta\alpha$ CH_2), and 1380 cm^{-1} (δ CH_3) due to various CH_2 bending modes of the lipid tails. Figure 3 shows that the relative intensity of bands due to the δ_s $^+N-CH_3$ mode for the $^+N(CH_3)_3$ headgroup increases with decreasing number of layers on TiO_2 surface.

This behavior in the change in relative intensity of the δ_s $^+N-CH_3$ mode is analogous to that observed for different cetyltrimethylammonium (CTAB) structures adsorbed on TiO_2.[29] Both DPPC and CTAB have the same positive headgroup moiety ($^+N(CH_3)_3$, see Figure 1), and thus we apply the same interpretation used previously for CTAB adsorbed on TiO_2[29] to explain the results for adsorbed DPPC shown in Figure 3. The direction of the transition dipole vector for the δ_s $^+N-CH_3$ band of an adsorbed lipid molecule (or CTAB) is normal to the surface.[30] In the case of CTAB, the intensity of this δ_s $^+N-CH_3$ band at 1396 cm^{-1} (A_{1396}) increases when the CTAB is bound directly to the surface through electrostatic interactions with negative charge sites on the surface.[29] Specifically, it was found that the ratio of A_{1396}/A_{2850} (A_{2850}: intensity of band at 2850 cm^{-1} that is proportional to the total amount of CTAB adsorbed on TiO_2) showed abrupt changes with different aggregated structures on the surface.[29] At low CTAB solution concentrations ($\sim 10^{-6}$ M), individual CTAB molecules adsorb on the surface leading to a high A_{1396}/A_{2850} ratio. In contrast, at concentrations above the critical micelle concentration (9×10^{-4} M), micelles adsorb on the surface. In this case, a low A_{1396}/A_{2850} ratio was obtained because only a small fraction of the CTAB molecules in the micelles are in direct contact with the surface.

By analogy to CTAB, the intensity of the 1396 cm^{-1} band in DPPC thus provides an indication of the number of lipid molecules directly contacted to the TiO_2 surface through electrostatic interactions. Because the intensity of the methylene tail band at 2850 cm^{-1} is insensitive to the packing structure of the lipid molecules, the intensity of the 1396 cm^{-1} band ratio to the 2850 cm^{-1} band (A_{1396}/A_{2850}) reflects the percentage of lipid molecules in the LB-deposited lipid architectures that interact directly with charge sites on the surface. Figure 4 shows a plot of the A_{1396}/A_{2850} ratio versus the number of LB layers deposited to TiO_2. The line in Figure 4 shows a decreasing trend in the relative intensity of the δ_s $^+N-CH_3$ band with the number of lipid layers deposited on the TiO_2 surface. Clearly, the trend in the A_{1396}/A_{2850} ratio is consistent with the percentage of DPPC molecules interacting with surface sites. The highest ratio would be expected for 1 layer, and this value would decrease with multilayer adsorption on the surface.

Interestingly, the A_{1396}/A_{2850} ratio could be used for identifying the DPPC lipid structures and in monitoring perturbations to the DPPC structures. An example is shown below where this ratio is used as an indicator to determine whether DPPC liposomes remain intact when adsorbed on TiO_2 or rupture to form a bilayer structure.

DPPC Liposome Adsorption on TiO_2. Figure 5 shows an ATR spectrum of the lipid adsorbed on the TiO_2 from a 5×10^{-3} M solution at pH 8.5 containing DPPC vesicles. A solution pH of 8.5 was chosen because at this pH, a maximum adsorbed amount of liposome is obtained. At solution pH values below 6.5, there is a dramatic decrease in the adsorbed amount of liposome. This confirms that the primary mode of interaction of the liposome with the surface is electrostatic between the cationic headgroup of the DPPC and the negative surface sites. We recall that the IEP of TiO_2 occurs at pH 6.6 and the surface is positively charged below this value.

Of the three spectra of LB film samples shown in Figure 2, the spectrum of the adsorbed DPPC vesicles most resembles the spectrum of the 5-layer LB sample. The spectrum of the 5-layer LB sample is replotted in Figure 5 for comparison. The ratio of A_{1396}/A_{2850} was calculated for adsorption from the liposome solution and is included in Figure 4. The position of these data points in Figure 4 suggests that the vesicle architecture remains intact when adsorbed on TiO_2. If the lipid vesicle structures had ruptured, we would anticipate a 2−3 layer structure on the surface and an A_{1396}/A_{2850} ratio > 0.25. This is not observed. Several QCM studies[6,8,18] show that when phosphotidylcholine lipid vesicles adsorbed on TiO_2, their vesicle architecture remains intact. This is consistent with the data obtained from the IR spectra.

In addition to the symmetric deformation vibration mode δ_s $^+N-CH_3$ band at 1396 cm^{-1}, the IR spectrum of CTAB contains bands at 1490 and 1479 cm^{-1} due to the antisymmetric deformation vibration modes δ_{as} $^+N-CH_3$ (see Figure 6a). These bands also provide structural information. As shown in Figure

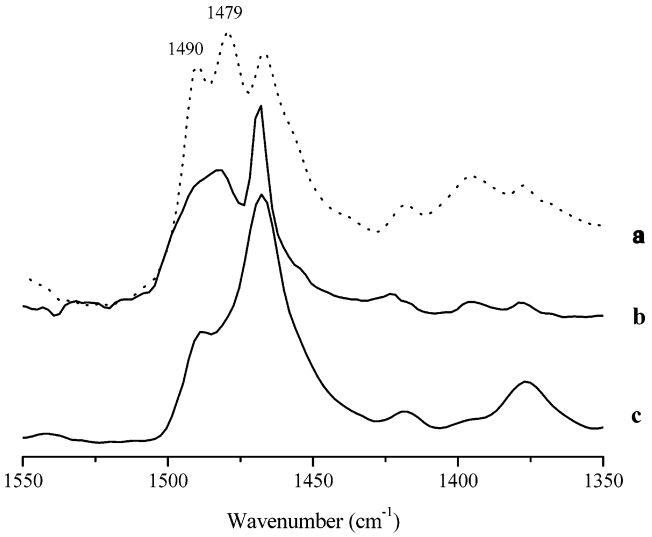

Figure 6. IR bands of the CTAB $^{+}N(CH_3)_3$ headgroup before (curve a) and after SDS addition (curve b) to a CTAB micelle adsorbed on TiO_2, and curve c is the $^{+}N(CH_3)_3$ headgroup spectrum of DPPC vesicles adsorbed on TiO_2.

1, the transition dipole vector for the δ_{as} $^{+}N-CH_3$ is orthogonal to that of the δ_s $^{+}N-CH_3$. Therefore, the δ_{as} $^{+}N-CH_3$ modes are sensitive to lateral interactions with counter charges. Again, we draw analogy to CTAB studies to determine structural information derived from the δ_{as} $^{+}N-CH_3$ bands. The changes occurring in the CTAB headgroup bands with addition of an anionic surfactant sodium dodecyl sulfate (SDS) have been reported in detail elsewhere.[16] Figure 6b shows the spectrum of the SDS addition to a CTAB micelle adsorbed on TiO_2. Approximately 63% of CTAB is ejected from the TiO_2 surface, and a mixed micelle with a CTAB/SDS ratio of 1.2 is formed. A lateral−lateral interaction between the SDS and CTAB is evidenced by the disappearance of the δ_{as} $^{+}N-CH_3$ bands at 1490 and 1479 cm^{-1}, giving rise to a broad ill-defined band at 1482 cm^{-1}. In Figure 6c, we have plotted the spectrum of DPPC vesicles adsorbed on TiO_2. This spectrum differs from the Figure 6a for CTAB micelles adsorbed on TiO_2 in that the δ_{as} $^{+}N-CH_3$ bands are broad and ill-defined, much like the spectrum of the mixed SDS/CTAB micelle. This is also the case for LB-deposited layers (see Figure 3). We therefore conclude that each $^{+}N(CH_3)_3$ headgroup is laterally interacting with the negatively charged PO_2^- of the adjacent DPPC molecule.

One of the advantages of using the ATR-FTIR technique is its ability to study the adsorption process dynamically. Figure 7 is a plot of the ratio of A_{1396}/A_{2850} as a function of contact time with the liposome solution. Spectra were recorded every 5 min during contact of the TiO_2-coated ATR with the flowing liposome solution. The inset figure is the relative amount of DPPC liposome adsorbed onto the TiO_2 computed using the intensity of the 2850 cm^{-1} band. Figure 7 shows an initial drop in the A_{1396}/A_{2850} ratio with contact time. It is noted that the total change is a small fraction of the line shown in Figure 4. The overall range for the change in the A_{1396}/A_{2850} ratio in Figure 7 is indicated by the hatched block area in Figure 4. This shows that during the entire adsorption process the adsorbed DPPC aggregates essentially retain their closed vesicle structures. However, Figure 7 does show some subtle structural changes as the rapid uptake of DPPC at the beginning of adsorption process is accompanied by a sharp decrease of the A_{1396}/A_{2850} ratio.

One possibility is that the first DPPC vesicles see a bare TiO_2 surface with many negative charge sites. As a result, the vesicles

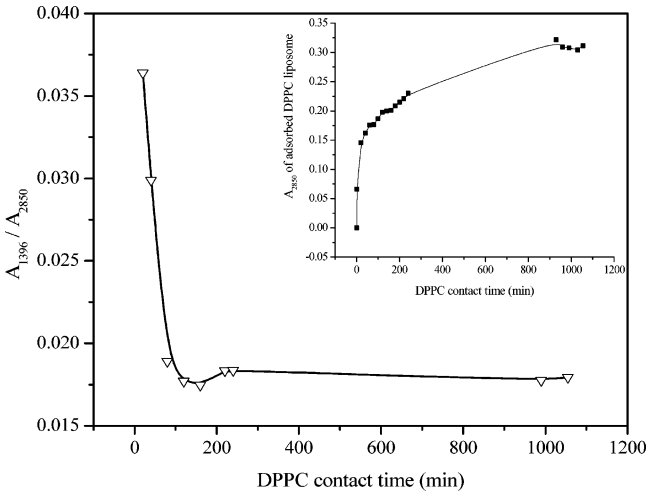

Figure 7. Relative intensity of the δ_s $^{+}N-CH_3$ band (A_{1396}/A_{2850}) as a function of contact time with the liposome solution. The relative change in the adsorbed amount of DPPC lipid on TiO_2 is shown in the inset.

flatten to a more ellipsoidal shape, adsorbing a higher number of DPPC molecules to charge sites per vesicle. As more vesicles adsorbed on the surface, the surface becomes more crowded and the existing vesicles adsorbed on the surface adopt a configuration with fewer average numbers of interactions with negatively charged sites to accommodate more vesicles on the surface.

Conclusions

Lipid structures on the TiO_2 surface obtained by LB deposition or by directly flowing the DPPC liposome solution across the TiO_2-coated ATR crystal have been investigated by ATR-FTIR spectroscopy. We found that the spectral changes associated with the headgroup vibrational modes can be used to identify the different lipid structures on TiO_2. In particular, we have shown that the bands due to PO_2^- modes are sensitive to changes in the degree of hydration of the LB films, whereas the symmetric deformation mode (δ_s $^{+}N-CH_3$) is sensitive to interaction with oppositely charged surface sites. Using this information, we found that the liposomes adsorbed on TiO_2 remain intact as vesicles and that the vesicles are stable and not removed by flowing water. We have also shown that the antisymmetric deformation vibration modes δ_{as} $^{+}N-CH_3$ are sensitive to changes in lateral−lateral DPPC interactions. This information was used to show that in DPPC aggregates adsorbed on TiO_2, each $^{+}N(CH_3)_3$ headgroup is interacting laterally with the negatively charged PO_2^- of the adjacent DPPC molecule.

Acknowledgment. This work was supported by the National Science Foundation (NSF) under Grant NSF BES0304523.

References and Notes

(1) Papahadjopoulos, D. *Liposomes & Their Uses in Biology & Medicine*; New York Academy of Sciences: New York, 1987.
(2) Banerjee, R. *J. Biomater. Appl.* **2001**, *16*, 3.
(3) Matsuura, M.; Yamazaki, Y.; Sugiyama, M.; Kondo, M.; Ori, H.; Nango, M.; Oku, N. *Biochim. Biophys. Acta* **2003**, *1612*, 136.
(4) Sackmann, E. *Science* **1996**, *271*, 43.
(5) Bouwstra, J. A.; Honeywell-Nguyen, P. L. *Adv. Drug Delivery Rev.* **2002**, *54*, 41.
(6) Reimhult, E.; Hook, F.; Kasemo, B. *Langmuir* **2003**, *19*, 1681.
(7) Hook, F.; Rodahl, M.; Keller, C.; Glasmastar, K.; Fredriksson, C.; Dahlqvist, P.; Kasemo, B. *Proc. Annu. IEEE Int. Freq. Contr. Symp.* **1999**, *2*, 966.
(8) Reimhult, E.; Hook, F.; Kasemo, B. *Phys. Rev. E* **2002**, *66*, 051905.
(9) Keller, C. A.; Glasmastar, K.; Zhdanov, V. P.; Kasemo, B. *Phys. Rev. Lett.* **2000**, *84*, 5443.

(10) Yang, B.; Furusawa, K.; Matsumura, H. *Langmuir* **2003**, *19*, 9023.
(11) Yang, B.; Matsumura, H.; Kise, H.; Furusawa, K. *Langmuir* **2000**, *16*, 3160.
(12) Reviakine, I.; Brisson, A. *Langmuir* **2000**, *16*, 1806.
(13) Egawa, H.; Furusawa, K. *Langmuir* **1999**, *15*, 1660.
(14) Puu, G.; Gustafson, I.; Artursson, E.; Ohlsson, P.-A. *Biosens. Bioelectron.* **1995**, *10*, 463.
(15) Yang, B.; Matsumura, H.; Katoh, K.; Kise, H.; Furusawa, K. *Langmuir* **2001**, *17*, 2283.
(16) Li, H.; Tripp, C. P. *J. Phys. Chem. B* **2004**, *108*, 18318.
(17) Groves, J. T.; Ulman, N.; Cremer, P. S.; Boxer, S. G. *Langmuir* **1998**, *14*, 3347.
(18) Reimhult, E.; Hook, F.; Kasemo, B. *J. Chem. Phys.* **2002**, *117*, 7401.
(19) Ninness, B. J.; Bousfield, D. W.; Tripp, C. P. *Colloids Surf., A* **2002**, *203*, 21.
(20) Yun, H.; Choi, Y.-w.; Kim, N. J.; Sohn, D. *Bull. Korean Chem. Soc.* **2003**, *24*, 377.
(21) Deo, N.; Somasundaran, P. *Colloids Surf., A* **2001**, *186*, 33.
(22) Ter-Minassian-Saraga, L.; Okamura, E.; Umemura, J.; Takenaka, T. *Biochim. Biophys. Acta* **1988**, *946*, 417.
(23) Umemura, J.; Cameron, D. G.; Mantsch, H. H. *Biochim. Biophys. Acta* **1980**, *602*, 32.
(24) Casal, H. L.; Mantsch, H. H. *Biochim. Biophys. Acta* **1984**, *779*, 381.
(25) Arrondo, J. L. R.; Goni, F. M.; Macarulla, J. M. *Biochim. Biophys. Acta* **1984**, *794*, 165.
(26) Wong, P. T.; Capes, S. E.; Mantsch, H. H. *Biochim. Biophys. Acta* **1989**, *980*, 37.
(27) Okamura, E.; Umemura, J.; Takenaka, T. *Vib. Spectrosc.* **1991**, *2*, 95.
(28) Okamura, E.; Umemura, J.; Takenaka, T. *Biochim. Biophys. Acta* **1990**, *1025*, 94.
(29) Li, H.; Tripp, C. P. *Langmuir* **2002**, *18*, 9441.
(30) Scheuing, D. R.; Weers, J. G. *Langmuir* **1990**, *6*, 665.